



Development of near-field optical/atomic-force microscope for biological materials in aqueous solutions

Hiroshi Muramatsu ^{a,*}, Norio Chiba ^a, Takeshi Umemoto ^a, Katsunori Homma ^a,
Kunio Nakajima ^a, Tatsuaki Ataka ^a, Satoko Ohta ^b, Akihiro Kusumi ^b,
Masamichi Fujihira ^c

^a *Research Laboratory for Advanced Technology, Seiko Instruments Inc., Takatsuka-shinden, Matsudo-shi, Chiba 271, Japan*

^b *Department of Life Sciences, Graduate School of Arts and Sciences, The University of Tokyo, Meguro-ku, Tokyo 153, Japan*

^c *Department of Biomolecular Engineering, Tokyo Institute of Technology, Nagatsuta, Midori-ku, Yokohama 227, Japan*

Received 9 May 1995; accepted 15 June 1995

Abstract

This paper reports improvements of optical fiber cantilevers and the scanning near-field optical microscopy imaging of biological materials in liquid. In our scanning near-field optical/atomic-force microscope (SNOAM), the scanning of an optical fiber cantilever over the specimen was controlled by dynamic mode AFM to reduce damage to the probe and soft specimens. The typical resonant frequency of the optical fiber cantilever was 19.5 kHz, while it was 23.0 kHz in air. The *Q*-factor of the cantilever depended on the vibration amplitude and was typically 260–600 in air and 40–240 in water. The relationship between the vibration amplitude and the average sample–probe separation indicated that the cantilever worked in the non-contact mode in water, while it worked in the cyclic-contact mode in air. Cultured cells in aqueous solutions were visualized by the SNOAM, indicating that the SNOAM is suitable to observe soft specimens.

1. Introduction

We previously developed a new scanning near-field optical microscope (scanning near-field optical/atomic-force microscope; SNOAM) in which a feedback signal from AFM in the dynamic mode was used to scan the probe tip along the surface contour of the sample [1,2]. An optical fiber with a sharp tip on one end was bent for use as a cantilever, and the AC amplitude of the cantilever deflection was held

constant during scanning by moving the stage. If this system operates successfully in liquids, it will be good for soft samples and those with great variations in height, such as cultured cells. In this sense, for observation of biological specimens, SNOAM may be superior to other systems that have been used in the atmospheric environment, such as those utilizing lateral shear force [3], STM [4], and contact-mode AFM [5,6] as a method to control sample–tip separation. Tapping mode AFM studies in liquids have been reported using flat type cantilevers [7–9] although the optical-fiber cantilever is round which helps to reduce viscous resistance.

In the present research, we improved the perfor-

* Corresponding author. Fax: +11 81 473 92 7822; E-mail: muramatu@tk.sii.co.jp.

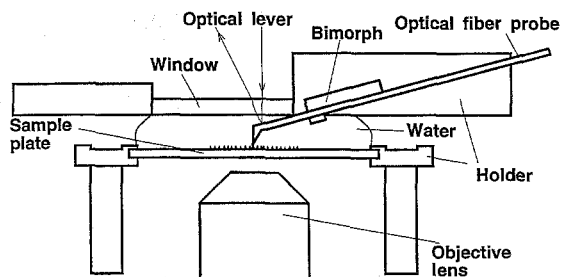


Fig. 1. Schematic diagram of the liquid cell in SNOAM system.

mance of the optical fiber cantilever and observed specimens in liquids. This paper reports the performance of the optical fiber cantilever and the observation of a standard specimen in liquid and displays near-field optical images of cultured cells in an aqueous solution.

Scanning near-field optical microscopy in liquids has been long-awaited for the observation of specimens in aqueous media and organic solvents with high resolution. In biology, optical microscopy is essential for studying the structural basis of functions of cells and supramolecular complexes because it allows observation of *their functional states in aqueous media*. However, the resolution of conventional (far-field) optical microscopy is typically several hundred nanometers, which is insufficient for observing molecular events. Electron microscopes have much better resolution, but do not allow observation in aqueous solutions.

2. Experimental setup

The SNOAM system is essentially the same as reported previously [2]. The optical-fiber cantilever

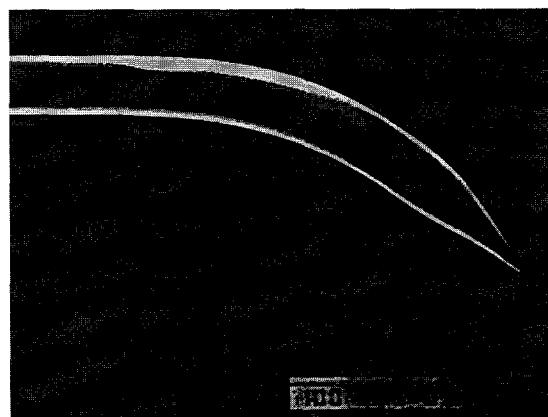


Fig. 2. Representative scanning electron microscope image of the probe made from an optical fiber coated with aluminum.

is mounted on a bimorph and vibrated vertically against the specimen stage at the resonant frequency (typically 10–40 kHz). The vibration voltage applied on the bimorph was between 0.5 and 10 V_{AC}. The vibration amplitude is monitored by detecting the deflection of the laser beam, which is reflected on the polished surface of the glass cantilever. The probe-sample distance is controlled dynamically by decreasing the vibration amplitude as the distance between the probe and the sample decreases.

Fig. 1 shows a liquid cell designed for the present experiment. Water and cell culture media were held between the glass plate and an upper window. Both the probe and the sample were immersed in solution.

The probe was prepared as described previously [2]. Briefly, an optical fiber was pulled with irradiation of a CO₂ laser to make a tip, and then bent with irradiation of a CO₂ laser. The probe was coated

Table 1

Resonant frequency (F) of the optical fiber cantilevers in air, water and glycerol solution of 2 and 4 cP

Optical fiber diameter (μm)	Media	F (Hz)	$F_{\text{media}}/F_{\text{air}}$ (%)	Viscosity of the media (cP)	Density of the media (g cm^{-3})	Calculated resonant frequency ratio (%)
125	Air	23.0	100	0.018	0.0012	100
125	Water	19.5	85	1	1	82.9
125	Glycerol solution	19.1	83	2	1.06	82.1
125	Glycerol solution	18.5	80	4	1.10	81.6
80	Air	18.8	100	0.018	0.0012	100
80	Water	16.5	88	1	1	82.9

with 200 nm thick aluminum, and an aperture was made at the tip during the vapor deposition (Fig. 2).

3. Results and discussion

The spring constant of the probe was 2–20 N/m as calculated on the basis of its shape (rod) and Young’s modulus for quartz glass. Typically, the resonant frequency of the optical fiber tip-cantilever was 23.0 kHz in air. The resonant frequency decreased to 19.5 kHz (85%) in water. The resonant frequency in glycerol solution of 2 and 4 cP shows a value similar to that in water as shown in Table 1. Also the 80 μm diameter optical fiber shows similar resonant frequency decrease although smaller cantilever normally takes larger viscous effect. This shows that the viscosity of the liquid affects only a little part of the resonant frequency change. Therefore this frequency decrease can be explained by an addition mass of water to the cantilever for the cantilever movement in liquid. This addition mass is estimated as $\pi\rho r^2 l$ where ρ is viscosity of liquid, and r and l are radius and length of rod cantilever, respectively. The resonant frequency is expressed roughly as $\omega = \sqrt{k/m}$, where m and k are the mass and spring constant of a vibrating material, respectively. The ratio of the resonant frequency in water

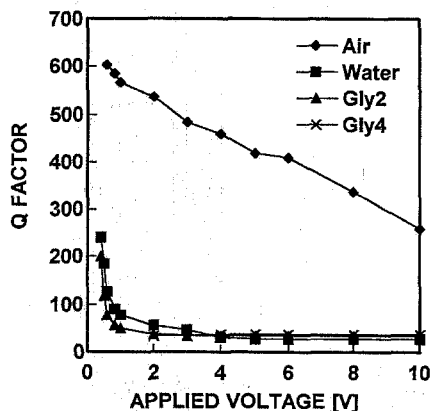


Fig. 3. Relationship between the Q -factor of the optical fiber cantilever and the applied voltage to the bimorph for the cantilever vibration.

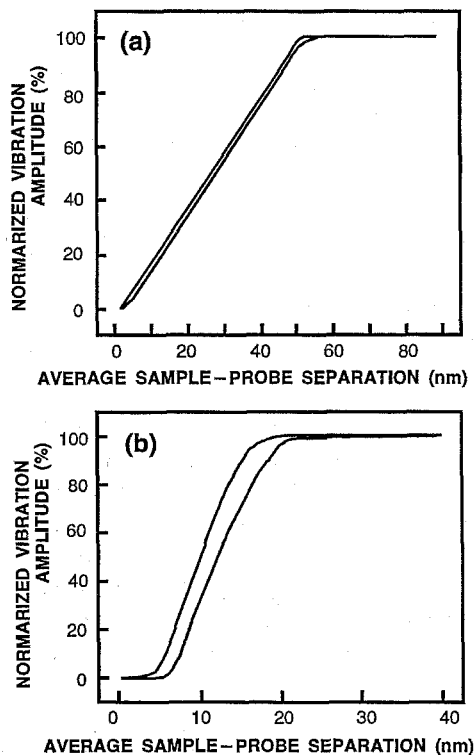


Fig. 4. Relationship between the vibration amplitude of the cantilever and the average sample–probe separation measured in air (a) and water (b). Vibration voltage of 1 V_{AC} was applied and the vibration amplitude is estimated 100 and 20 nm for air and water, respectively, from this relation.

versus that in air can be estimated using the addition mass of water as shown in the following equation.

$$\frac{\omega_{\text{water}}}{\omega_{\text{air}}} = \frac{\sqrt{k/(m_{\text{cantilever}} + m_{\text{water}})}}{\sqrt{k/m_{\text{cantilever}}}} = \frac{\sqrt{\pi\rho_{\text{quartz glass}} r^2}}{\sqrt{\pi\rho_{\text{quartz glass}} r^2 + \pi\rho_{\text{water}} r^2}} = 0.829,$$

where $\rho_{\text{quartz glass}}$ and ρ_{water} are 2.2 and 1.0 g cm⁻³ at 20°C, respectively. This value (83%) agrees with the experimental result (85%).

Fig. 3 shows the relationship between the Q -factor and the voltage applied on the bimorph to vibrate the cantilever. The Q -factor is decreased by a factor of about 5–8 when the cantilever was immersed in water. The Q -factor also depended on the vibration

amplitude as shown in Fig. 3. This dependence is much larger in water than in air. This is because the viscous resistance is larger in water than in air, i.e. the kinematic viscosity of air and water is 0.150 and 1.00 St at 20°C, respectively. The Q -factor in the glycerol solutions shows smaller value than that in water at the applied voltage smaller than 1 V_{AC} . But the Q -factor shows almost similar value in water and glycerol solutions over 2 V_{AC} of applied voltage. This means the amplitude or velocity of cantilever vibration dominates the Q -factor in this region. This Q -factor is sufficient to operate non-contact-mode AFM in water.

The AC voltage that must be applied to the bimorph to obtain a curve in water similar to that in air is greater by a factor of about 7 in water. The maximum vibration amplitude is proportional to the vibration voltage applied to the bimorph. With a decrease in the sample–probe separation, the vibration amplitude decreases as the probe approaches the sample at the extreme of each vibration cycle.

The relationship between the vibration amplitude

of the cantilever and the average sample–probe distance was measured in air and water by varying the height of the specimen stage (Fig. 4). Fig. 4a shows that the amplitude decreases linearly in air. Linear decrease of the vibration amplitude with lowering of the sample position outside the roll-out point is characteristic of the cyclic-contact-mode AFM and indicates that cyclic-contact-mode AFM operates normally in air. The actual vibration amplitude can be estimated from this curve because the vibration amplitude decreases due to the decrease of vibration space of the probe, i.e. the distance between the roll-up point of the average sample–probe separation and 0% point of that corresponds to half of the actual vibration amplitude. In the case of Fig. 4a, the vibration amplitude was 100 nm for applying 1 V_{AC} to the bimorph.

Fig. 4b shows that the amplitude decreases more gradually in water than in air. Gradual decrease of the vibration amplitude with lowering of the sample position outside the roll-out point is characteristic of the non-contact-mode AFM and indicates that non-

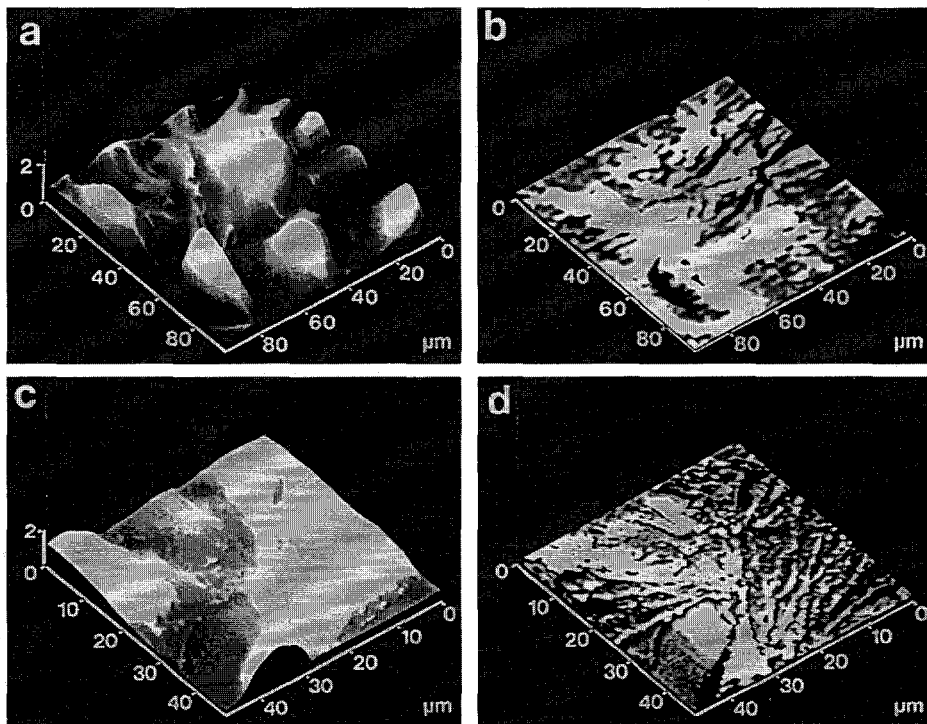


Fig. 5. Topographic (a, c) and near-field (b, d) images of cultured normal rat kidney (NRK) fibroblasts in an aqueous solution. The cells were fixed by cross-linking with 2% paraformaldehyde. The areas imaged are 100 $\mu\text{m} \times 100 \mu\text{m}$ (a, b) and 50 $\mu\text{m} \times 50 \mu\text{m}$ (c, d).

contact-mode AFM operates normally in water. The steep part of the curve indicates that the cantilever is in the cyclic-contact (tapping) mode. The amplitude at the roll-out point is proportional to the vibration voltage between 1 and 10 V_{AC} . The oscillation amplitude employed was between 20 and 200 nm (1–10 V_{AC} for driving the bimorph) in water. The large oscillation amplitude is due to the long cantilever, which is 2–4 mm long, while normal cantilever probe for non-contact AFM is 100–500 μm long and shows a vibration amplitude of 10–20 nm in air.

Under typical imaging conditions, average sample–probe separation was controlled so that the amplitude of the vibration became 98% of the maximum vibration (when the probe was placed far away from the sample, the range of maximum vibration amplitude employed was between 20 and 200 nm). Therefore, the interaction force between the probe and the sample is likely to be as small as that for normal tapping mode AFM in water.

Spatial resolution was examined by using a 1 $\mu\text{m} \times 1 \mu\text{m}$ checkered pattern made with 20 nm thick chromium coating over a quartz plate. The topographic and optical images were examined clearly near the edge of chromium coating. Because the edges of the chromium patterns are thinner than 100 nm, the resolution of SNOAM is estimated to be better than 100 nm in topographic and optical images.

Figs. 5a and 5b show representative topographic and optical images of normal rat kidney (NRK) fibroblasts in culture obtained simultaneously with the non-contact AFM mode and near-field optical transmission mode. This cell line was cultured on a 22 mm \varnothing cover slip. The cells were fixed with 2% paraformaldehyde before SNOAM observation. Overall topography of the cell in lower magnification (Fig. 5a) is similar to that obtained for living fibroblasts by contact-mode AFM in a cell culture medium [10]. The outer edges of the cells coincided in the near-field and non-contact-mode AFM topographic images, while the fine structures observed in the near-field image are different from the topographic image.

Figs. 5c and 5d show the images at a higher magnification. The near-field image (Fig. 5d) shows many stress fiber-like filamentous structures in the cell, while the topographic image is weakly sensitive to such structures. These filaments are difficult to

observed in normal Nomarski and phase-contrast optical microscopy due to the lower resolution and contrast. But similar structures were also observed in the contact-mode AFM images.

Various filaments inside living cells can be visualized from outside the cells using the *contact-mode* AFM, while topographic images of the cell by SNOAM (Figs. 5a and 5c) exhibited only the surface of the cell. This result further demonstrates that the force exerted by the probe on the cell membrane is substantially weak.

Thus, SNOAM introduces a new method for studying cellular structures in living cells at a resolution and contrast unobtainable by conventional optical microscopy. This technique may reveal cell characteristics hitherto undetected by optical microscopy of living cells or electron microscopy of processed cells. In addition, the present study suggests that the SNOAM system is widely applicable to specimens in water and other fluid media.

Acknowledgements

This study was supported in part by Special Coordination Funds from the Science and Technology Agency of the Japanese government.

References

- [1] H. Muramatsu, N. Chiba, T. Ataka, H. Monobe and M. Fujihira, *Ultramicroscopy* 57 (1995) 141.
- [2] N. Chiba, H. Muramatsu, T. Ataka and M. Fujihira, *Jpn. J. Appl. Phys.* 34 (1995) 321.
- [3] E. Betzig and J.K. Trautman, *Science* 257 (1992) 189.
- [4] U.T. Dürig, D.W. Pohl and F. Rohner, *J. Appl. Phys.* 59 (1986) 3318.
- [5] S. Shalom, K. Lieberman and A. Lewis, *Rev. Sci. Instr.* 63 (1992) 4061.
- [6] N.F. van Hulst, M.H.P. Moers, O.F.J. Noordman, R.G. Tack, F.B. Segerink and B. Bölger, *Appl. Phys. Lett.* 62 (1993) 461.
- [7] P.K. Hansma, J.P. Cleveland, M. Radmacher, D.A. Walters, P.E. Hillner, M. Bezanilla, M. Fritz, D. Vie and H.G. Hansma, *Appl. Phys. Lett.* 64 (1994) 1738.
- [8] C.A.J. Putman, K.O. van der Werf, B.G. de Groot, N.F. van Hulst and J. Greve, *Appl. Phys. Lett.* 64 (1994) 2454.
- [9] M. Dreier, D. Anselmetti, T. Richmond, U. Dammer and H.J. Güntherodt, *J. Appl. Phys.* 76 (1994) 5095.
- [10] M. Takeuchi, H. Miyamoto, H. Komizu and A. Kusumi, *Cell Struct. Funct.* 17 (1992) 487.